Proton Damage Comparison of an e2v Technologies N-channel and P-channel CCD204

J. P. D. Gow, N. J. Murray, A. D. Holland and D. Burt

Abstract— **Comparisons have been made of the relative degradation of charge transfer efficiency in n-channel and p-channel CCDs subjected to proton irradiation. The comparison described in this paper was made using e2v technologies plc. CCD204 devices fabricated using the same mask set. The device performance was compared over a range of temperatures using the same experimental arrangement and technique to provide a like-for-like comparison. The parallel transfer using the p-channel CCD was then optimised using a trap pumping technique to identify the optimal operating conditions at 153 K.**

Index Terms—**CCD, p-channel, proton radiation damage, charge transfer inefficiency, pocket/trap pumping**

I. Introduction

THE initial radiation damage assessment performed for the European Space Agency (ESA) mission Euclid used a front illuminated n-channel CCD204 [1]. Experimental analysis and modelling provided inputs for discussion between the Euclid consortium and e2v technologies plc. in respect of device optimisation, leading to the development of the CCD273 [2, 3]. Part of the program also included the development of p-channel CCD's produced using the same mask set as the CCD204, to investigate the possibility of using such a device type for the mission.

Euclid's primary mission objective is to perform a study of the geometry and nature of the dark Universe using several techniques of investigation, including weak gravitational lensing [4]. This technique measures the change in ellipticity of galaxies, to the order of a few percent, which allows the mass distribution to be constructed. To accomplish this requires a large survey and an extremely accurate measurement of the galaxy shapes. The radiation induced increase in charge transfer inefficiency (CTI) will lead to the introduction of a systematic error on this measurement, making it essential to understand and minimise the impact of the space radiation environment. A significant amount of work has been performed and continues to be performed within the Euclid visible imager consortium to ensure this understanding and optimal device performance is achieved [1, 3, 5-7].

The benefit of using p-channel CCDs to achieve greater displacement damage hardness was originally demonstrated in 1997 [8] and a number of other studies have demonstrated an improved tolerance to radiation-induced CTI when compared to n-channel CCDs [9-14], therefore the use of a p-channel CCD was considered for Euclid. However, due to the test readiness level of a suitable p-channel CCD the n-channel CCD273 was selected and the work on p-channel CCDs decoupled from the Euclid programme.

The aim of the initial comparison using the CCD204 was to perform a like-for-like experimental comparison of n-channel and p-channel CCDs, to investigate the questions raised by Lumb 2009 [15]. This paper highlighted the complications which arise when attempting to make comparisons using different measurement techniques and made the recommendation that tests should be performed for a specific application, using "the appropriate operating modes and signal levels" [15]. The other aim of this initial investigation was to provide input into a future more detailed study

An earlier attempt was made to use similar operating conditions to an n-channel CCD02 using the e2v technologies p-channel CCD47 [14]. However, due to the poor pre-irradiation performance of the p-channel CCD47 the clocking scheme used was different. Although the study demonstrated the ability of a p-channel CCD to be more radiation hard than an n-channel CCD, the poor initial performance of the device made analysis difficult and the study failed to address the questions raised by Lumb [15].

The poor pre-irradiation performance of the p-channel CCD47 was attributed to its manufacture on epitaxial silicon [14]. Bulk (float zone) material having demonstrated comparable base CTI equivalent to n-channel devices [10, 13] the two batches of back-illuminated p-channel CCD204s were manufactured using high resistivity bulk n-type silicon and thinned to ~70 μm. Due to the availability of material, batch #10092 was manufactured on standard single side polished wafers and batch #10152 on double side polished wafers.

The radiation damage analysis performed using the n-channel CCD204 used mission appropriate readout rates and clocking schemes, detailed in the experimental section, with data collected over a range of temperatures. The initial study using the p-channel CCD204 would mirror those tests performed using the n-channel CCD204, including the

Manuscript received month date, year. This work was supported in part by ESA, e2v technologies plc., and the Centre for Electronic Imaging.

J. P. D. Gow, N. J. Murray and A. D. Holland are with the Centre for Electronic Imaging, Planetary and Space Sciences, The Open University, MK7 6AA, UK (e-mail: jason.gow@open.ac.uk)

D. Burt is with e2v technologies plc., Chelmsford, CM1 2QU, UK (email: david.burt@e2v.com)

assessment of cosmetic quality, dark current and the CTI measurements made using the X-ray technique as a function of CCD temperature.

Upon the completion of this study before the devices were returned to ESA an investigation was performed using the trap pumping technique [5, 16, 17] on the most damaged device to investigate methods for possible improvement to parallel charge transfer. The results from this study are also described.

II. Background

As a result of the temperature dependence of trap behaviour and the probability that the charge packet could encounter a trap, there are a number of difficulties which arise when making a comparison using different measurement techniques, operating temperatures, clocking and device structures [15].

The capture and emission of electrons and holes can be described by Shockley-Read-Hall theory [18-19], where the probability of capture and emission relate respectively to the capture time constant, τ_c, and the emission time constant, τ_e. The measured CTI is closely linked to τ_e of different traps. The CTI will be low [1] if either the τ_e is very much less than the time allowed for trapped charge to rejoin the charge packet, t_r, or if the τ_e is very much greater than the mean time between successive X-ray events, t_x. Therefore the impact of a particular trap species on the movement of charge within a CCD is dependent on clock timings and temperature. Similar CTI profiles can be created by changing either clock timings or temperature, i.e. moving in and out of a region where a specific trap is dominating CTI.

The method with which the CCD is operated will also impact the behaviour of charge during readout. The probability of charge being trapped is linked to the amount of charge under an electrode, and will vary depending on the number of traps present [7]. Therefore an increase in the image integration time will result in a greater number of empty traps in regions of the device containing little charge, effectively awaiting charge from an incident photon to pass and be captured. The disposition of charge within the CCD will also affect the measurement, for example a reduction in the number of X-rays incident on the CCD will result in decreased CTI and although CTI measurements made using the extended pixel edge response and X-ray techniques will follow a similar trend the actual CTI values will be different.

These are some of the complications which arise when making comparisons between data where operating temperature, charge distribution within the CCD and clock timings are not identical. Hence the benefit of performing a like-for-like study to remove some of these complications, leaving only the behaviour of the different trap species affecting n-channel and p-channel charge transfer. It should be noted that the n-channel CCD204 was front illuminated and the p-channel CCD204 back illuminated, this should not have an impact on CTI measurements as the 5,898 eV X-rays are sufficiently penetrating.

The CCD204 is 1064 by 4096 12 μm square pixel device with a 50 μm wide register channel width to allow for the option of on-chip pixel binning. The CCD204, illustrated in Figure 1, utilises four phase image clocks and three phase register clocks. Unlike the CCD203, previously flown onboard the Solar Dynamics Observatory launched in 2010, on which it is based it benefits from having a charge injection structure. The CCD204 is a non-inverted mode operation device, and does not include a supplementary buried channel.

III. Experimental

The same physical experimental setup was used as previously employed for n-channel testing [1], illustrated in Figure 2, with the p-channel CCDs mounted onto a copper cold bench in the same camera system using the same headboard. To allow the same headboard to be used, additional circuitry was incorporated to invert the clocks and video output and provide negative bias.

Cooling was provided by a CryoTiger® refrigeration system with the temperature controlled using a feedback system, comprising a Lakeshore 325 temperature controller, platinum resistance thermometer (PRT) mounted onto the copper cold bench, and a heater. A second PRT was mounted onto the CCD package to provide the operating temperature, it is assumed that the device silicon is in good thermal contact with the package.

An XTF5011/75-TH X-ray tube was used to fluoresce a polished manganese target held at 45° to the incident X-ray beam to provide a controllable number of 5,898 eV X-rays onto the CCD. Event re-combination code was used to combine split events for the purpose of counting the number of X-rays incident onto the detector. The manganese target was held at a distance to provide a uniform X-ray exposure at the CCD, and the vacuum bellows allows for minor adjustments to be made. Clocking and biasing was provided by an XCAM ltd. USB2REM2 camera drive box in conjunction with drive software controlled use a custom MatLab software program.

The same integration time (500 s), pause between image acquisition (90 s), clocking scheme (a parallel phase transfer time of 14.4 μs and with the CCD readout at 200 kHz) and X-ray flux (1 event per 80 pixels) were used to make the comparison. The X-ray flux was selected to provide an equivalent amount of charge to that which would be deposited within a typical Euclid image, to provide an indication of trends in CTI behaviour.

The n-channel and p-channel devices were irradiated at the Kernfysisch Versneller Instituut (KVI) in Holland, the 10 MeV equivalent proton fluence delivered to the devices is given in Table 1. A shield was placed over the CCDs during the irradiation to provide on-chip controls. It should be noted that only limited tests were performed on the n-channel CCDs prior to irradiation, the p-channel CCD204s benefited from a complete characterisation pre and post irradiation.

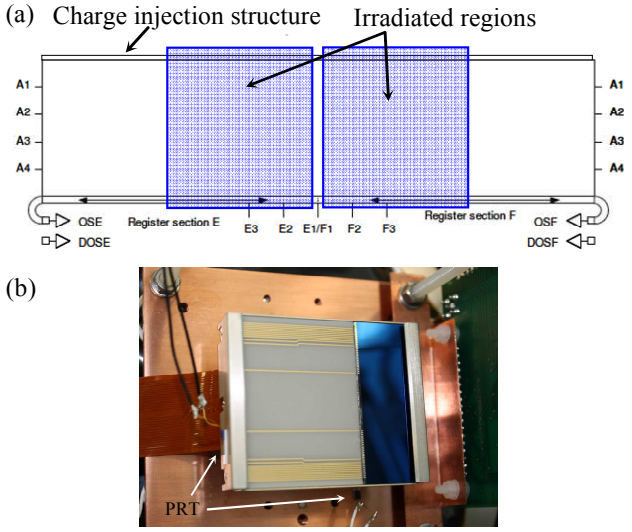

Fig. 1. Schematic showing the irradiated regions (a) and photograph (b) of the e2v technologies CCD204-22, the photograph shows the CCD204 mounted onto a copper cold bench as part of the CEI test camera and shows the position of the two PRTs.

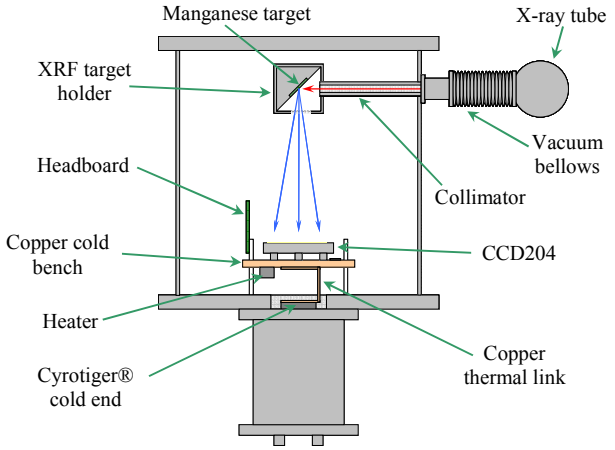

Fig. 2. Schematic of the experimental setup with the CCD204 mounted onto a copper cold bench and X-rays fluoresced from a manganese target to provide a controllable number of 5,898 eV X-rays onto the CCD.

IV. Results

A. Cosmetic Quality

During pre-irradiation testing it quickly became apparent that these devices were a significant improvement from the p-channel CCD47 The devices from batch #10152, produced using double sided polished wafers (these are not normally used for CCD production, but were available from another programme), however suffered from increased trap density. This resulted in the poor cosmetic quality, illustrated in Figure 3.

TABLE I
Proton Irradiation Details

Device	Region	10 MeV equivalent fluence (protons.cm^{-2})
05316-07-02	AE	4.0×10^{9}
	AF	2.0×10^{9}
05325-03-02	AE	4.0×10^{9}
	AE	8.0×10^{9}
10092-02-03	AE	2.0×10^{9}
	AF	4.0×10^{9}
10152-01-03	AE	8.0×10^{9}
	AF	1.0×10^{10}
10092-02-02	AE	5.0×10^{10}
	AF	1.0×10^{11}

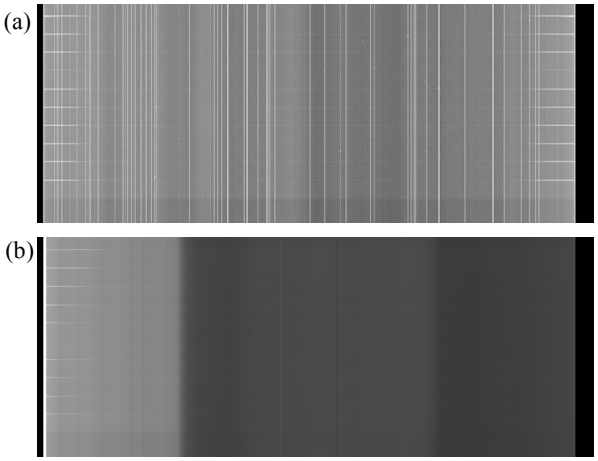

Fig. 3. Dark image taken at room temperature taken with device #10152-01-03 (a) and #10092-02-02 (b), with 1/10th second frame integration and ~23 second readout. The horizontal lines at the edge of the images are charge injection and the vertical lines are smeared out point defects.

B. Dark Current

The pre-irradiation dark current was found to be around twice that of the n-channel CCD204, being around 3 nA.cm^{-2} at room temperature. However, the n-channel CCD204 is front illuminated while the p-channel CCD204 is back illuminated. N-channel back illuminated CCDs have a typical dark current of between 2-3 nA.cm^{-2} at room temperature, therefore the pre-irradiation dark current of the back illuminated p-channel CCD204 appears to be comparable.

The activation energy, E_{act}, was measured post irradiation using the approximation in equation 1, where A is some constant, k is the Boltzmanns constant and T is the temperature [19]. It was found to be between 0.61 eV and 0.63 eV. These results are comparable to other reported values for p-channel CCDs [10, 12, 14]. It should be noted that only data collected above 180 K was used during this analysis.

$$Dark\ Current = A\exp\left(\frac{-E_{act}}{kT}\right) \quad (1)$$

The read noise, arising from the CCD, measured using the n-channel and p-channel CCDs was found to be comparable,

the noise on the p-channel CCD204 was calculated to be 1.4 h^+ r.m.s. at 160 K and 1.3 e^- r.m.s. at 160 K for the n-channel CCD204.

C. Charge Transfer Inefficiency

A region of interest (ROI) was selected that contained either un-irradiated or irradiated pixels; these regions are illustrated in Figure 1. The ROI was then divided into bins 40 pixels wide to identify X-ray event locations to be used in the measurement of parallel and serial CTI respectively. Analysis code was then used to collect event location information from a number of images. The peak location within each bin was identified by fitting a Gaussian to the X-ray events within that bin and the CTI measured using the gradient of the line of best fit applied to the data and the X-ray signal X(e-), in the form [16]

$$CTI_X = \frac{S_D(e^-)}{X(e^-)n_t} \quad (2)$$

where S_D(e-) is the average deferred charge, and n_t is the number of pixels transfers. The error on the CTI was calculated using the error on the weighted mean of the peak location and the error on the gradient, found using a parallelogram of error. The error from the equipment is taken as ± 2 ADC channels. The measurement of CTI using X-rays is described as an absolute measurement of CTI [16].

The pre-irradiation parallel CTI is illustrated in Figure 4, showing the trend as a function of temperature. An indication of the defect which could be responsible is also illustrated, based on the emission time constants calculated by Mostek et al. 2010 [17]. Both the serial and parallel CTI were comparable to those measured using an n-channel CCD, demonstrating a clear improvement in device manufacture and material selection at e2v over that used previously [9, 14] and believed to be as a result of using bulk material. The poor CTI of batch #10152 at around 170 K is believed to be as a result of using doubled side polished wafers, leading to an increase in the number of defects present within the CCD through no back-surface getter being present. The cosmetic quality of devices from batch #10152 was also poor when compared to those from batch #10092, the latter being comparable to n-channel CCDs.

Post irradiation there was a clear increase in CTI as a result of the creation of stable defects within the silicon lattice. When comparing the measured CTI values with those of the n-channel CCD204s, the increase in p-channel CTI was found to be greater at some temperatures. To enable a comparison the radiation damage constant (RDC), given by

$$RDC = \frac{\Delta CTI}{10\,MeV\ proton\ fluence} \quad (3)$$

was calculated for both the n-channel and p-channel devices. These values were compared by calculating the factor of

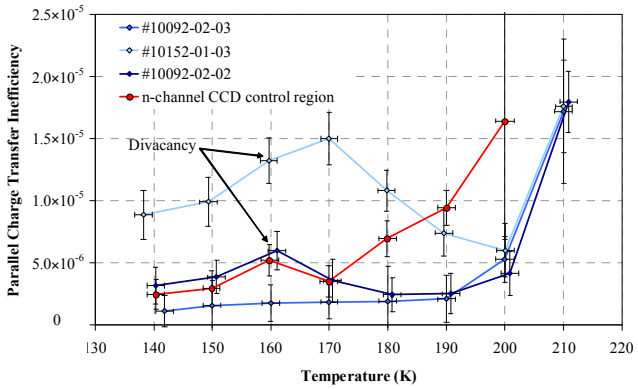

Fig. 4. Parallel CTI measured using three p-channel CCD204 devices pre-irradiation as a function of temperature. The CTI measured using the control region of an n-channel CCD204 is also included. The defects which could be responsible for the observed trend are also included, based on the emission time constants reported by Mostek et al. 2010 [17].

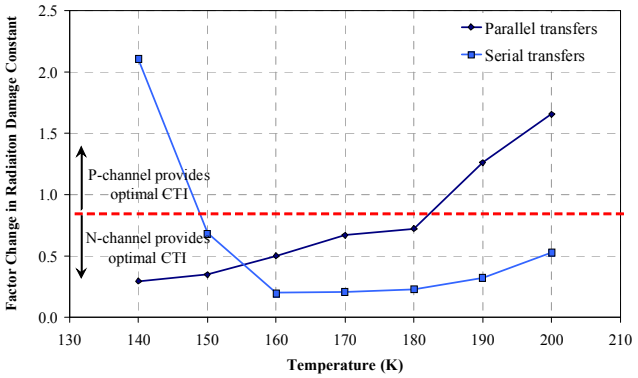

Fig. 5. Comparison of the difference in parallel and serial RDC values for the n-channel and p-channel CCD204 devices examined. A factor of 1 would indicate comparable performance. The observed trend is linked to operating timings and their relationships to different trap species which affect n-channel and p-channel CCD operation.

change, given by

$$Factor\ of\ Change\ in\ RDC = \frac{RDC_{n-channel}}{RDC_{p-channel}} \quad (4)$$

and illustrated in Figure 5, where a factor of 1 is comparable performance. It is evident that under these operating conditions the p-channel CCD would only offer improved performance when compared to an n-channel CCD at 140 K for serial transfers and 190-200 K for parallel transfers.

The reason for the observed trend is primarily due to the selection of the operating conditions, which were selected for Euclid based on the mission requirements and many years of experience operating n-channel CCDs. As the temperature of the n-channel CCD is reduced, the time allowed for the charge to rejoin the charge packet, t_r, for serial transfer approaches the emission time constant of the A-centre defect. This results in increased serial CTI below 160 K. At this readout speed and temperature, the p-channel CCD is not as strongly affected by a defect and it will therefore out-perform an n-channel equivalent.

When the temperature is increased, the time between successive X-ray events, t_x, for parallel transfer in the n-channel CCD approaches the emission time constant of the E-centre defect, resulting in the an increase in parallel CTI. The trend observed using the p-channel CCD is not strongly affected by a defect at higher temperatures, which results in the observed improvement in parallel CTI in Figure 5 when compared to an n-channel CCD.

Using values for the emission time constants of hole traps [17] and comparing these to the parallel timings, it is evident that the parallel t_r is comparable to the emission time constant of the divacancy, illustrated in Figure 6. The trap pumping technique was used with the device held at 153 K to quickly investigate the suppression of traps affecting parallel transfer by reducing the parallel transfer rate, effectively increasing t_r. This was achieved by increasing the image clock pulse edge overlap from 14.4 µs, referred to as toi, and counting the number of bright and dark pixel dipoles [5].

The CTI was then measured as a function of toi using device #10092-02-02 held at 153 K, illustrated in Figure 7. The parallel CTI in Figure 7 demonstrates a clear decrease with increasing toi, which from Figure 4, is believed to be a result of increasing t_r with respect to the divacancy emission time constant at 153 K. The range in the divacancy emission time constant from Mostek *et al.* 2010 [17] is included in Figure 6, showing a clear correspondence with the improvement in parallel CTI. Increasing the toi to 500 µs resulted in a reduction in the CTI from 1.9×10^{-3} to 2.0×10^{-4} at 153 K.

After a 10 MeV equivalent proton fluence of 1×10^{11} protons.cm^{-2} the parallel CTI of an n-channel CCD204 operated using the same parameters as in Gow et al. 2012 [1] was calculated, using a linear fit to the data, to be 1.1×10^{-3} at 153 K. Assuming a comparable improvement in performance as reported by Murray *et al.* 2012 [5], this could be reduced to 7.0×10^{-4} through an optimisation of the parallel transfer. However, the p-channel device, after a brief optimisation, is capable of providing a CTI value of 2.0×10^{-4}. Clearly indicating that p-channel CCDs will play a vital role in future systems intended for operation in hostile radiation environments, subject to the mission specific operating requirements.

Due to the nature of the defects affecting operation it is evident that using p-channel CCDs will allow operation at warmer temperatures, i.e. avoiding the need to cool the device to freeze out the E-centre defects which strongly impact CTI in n-channel devices. Only the limits imposed by a specific scientific goal can really decide which device can outperform another.

V. Conclusions

The latest e2v technologies plc. p-channel CCD has achieved comparable base performance to that of an n-channel CCD.

Although the points raised by Lumb 2009 [15] on comparing devices using the same techniques remain valid, it is important to operate a device using the best available information from the literature and to perform sufficient investigation to achieve device specific optimal performance.

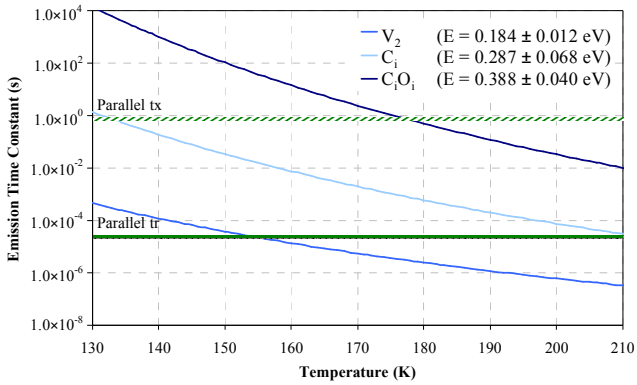

Fig. 6. Hole emission time constants calculated as a function of temperature by Mostek *et al.* 2010 [17]. The approximate time between X-ray events and the approximate time charge can rejoin the charge packet is also included, indicating the strong effect the divacancy has on parallel charge transfer.

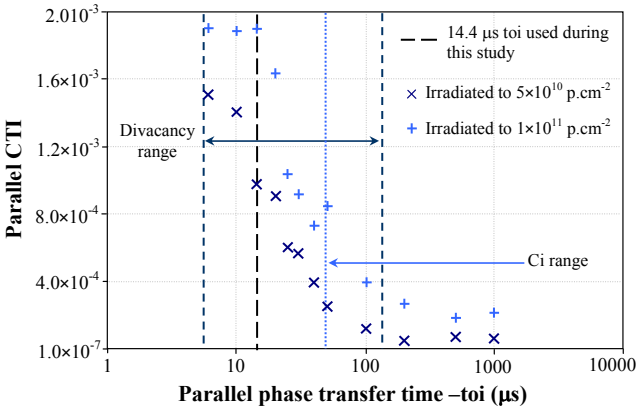

Fig. 7. Parallel CTI measured using device #10092-02-02 as a function of toi measured at 153 K. The range in the divacancy emission time constant from the values reported by Mostek *et al.* 2010 [16] clearly shows the effect of moving away from the divacancy defect emission time constant.

In the case of parallel CTI at 153 K, a slow transfer speed has been demonstrated to be optimal, to increase the probability that trapped charge will rejoin the charge packet. A considerable amount of work is required to investigate the trap behaviour within these devices, to both provide optimal operating conditions and to further our understanding of the effect hole traps have on CCD operation. This future work will include; a detailed study of device optimisation, which could not be performed during this short study; a complete electro-optical characterisation; a cryogenic irradiation; the development of a 3D device model and a Monte Carlo charge transfer model to investigate trap species and evaluate their density both pre and post proton irradiation.

The selection of a p-channel CCD for the Euclid visible imager is no longer feasible due to the time required to perform a complete electro-optical characterisation of the detector. Euclid will instead use an n-channel CCD273 [2, 3]. Based on the parallel CTI of the CCD273 at 153 K, after the Euclid end of life 10 MeV equivalent proton fluence of

4.8×10^{9} protons.cm^{-2} reported in Gow *et al.* 2012 [3], a p-channel CCD273 could offer a factor of ×5 improvements in parallel CTI. This reduces to a factor of ×3 when using the optimisation to n-channel parallel transfer reported by Murray *et al.* 2012 [5]. These improvements in performance are comparable to other reported values for p-channel CCDs.

As described there are a number of difficulties which arise when trying to compare the performance of different devices, if attempting to account for different measurement techniques and operating conditions. It would be advisable to compare the performance of each different technology for mission specific applications, using the optimal operating conditions. However, as our understanding of the radiation damage effects experienced by imaging device increases this should allow for the production of a set of rules to ensure an appropriate n-channel or p-channel CCD or Complementary Metal-Oxide-Semiconductor Image Sensor is selected.

ACKNOWLEDGMENT

The authors would like to thank e2v technologies plc. (in particular Steve Darby and James Endicott), and ESA (in particular Ludovic Duvet) for their support during this programme.

REFERENCES

[1] J. P. D. Gow, N. J. Murray, A. D. Holland, et al., "Assessment of space proton radiation-induced charge transfer inefficiency in the CCD204 for the Euclid space observatory", Journal of Instrumentation, vol. 7, 2012.

[2] J. Endicott, S. Darby, S. Bowring, et al., "Charge-coupled devices for the ESA Euclid M-class mission", *Proc. SPIE*, 2012, vol. 8453.

[3] J. P. D. Gow, N. J. Murray, D. J. Hall, et al., "Assessment of proton radiation-induced charge transfer inefficiency in the CCD273 detector for the Euclid Dark Energy Mission", *Proc. SPIE*, 2012, vol. 8453.

[4] M. Cropper, A. Refregier, P. Guttridge, et al., "VIS: the visible imager for Euclid", *Proc. SPIE*, 2010, vol. 7731.

[5] N. J. Murray, A. D. Holland, J. P. D. Gow, et al., "Mitigating radiation-induced charge transfer inefficiency in full-frame CCD applications by 'pumping' traps", *Proc. SPIE*, 2012, vol. 8453.

[6] D. J. Hall, A. D. Holland, N. J. Murray, et al., "Modelling charge transfer in a radiation damaged charge coupled device for Euclid", *Proc. SPIE*, 2012, vol. 8453.

[7] D. J. Hall, N. J. Murray, A. D. Holland, et al., "Determination of in situ trap properties in Charge Coupled Devices using a single-trap "pumping" technique", *RADECS*, 2013.

[8] J. P. Spratt, B. C. Passenheim and R. E. Leadon, "The Effects of Nuclear Radiation on P-channel CCD Imagers*", IEEE Radiation Effects Data Workshop*, 1997, pp. 116-121.

[9] G. R. Hopkinson, "Proton damage effect on P-channel CCDs", IEEE Trans. Nucl. Sci., vol. 46, no. 6, pp. 1790-1796, 1999.

[10] C. Bebek, D. Groom, S. Holland, et. al., "Proton Radiation Damage in P-channel CCDs Fabricated on High-Resistivity Silicon", IEEE Trans. Nucl. Sci., vol. 49, no. 3, pp. 1221-1225, 2002.

[11] C. Marshall, P. Marshall, A. Wczynski, et al., "Comparisons of the proton-induced dark current and charge transfer efficiency responses of n- and p-channel CCDs", *Proc. SPIE*, 2004, vol. 5499.

[12] J. P. Spratt et al., "Proton Damage Effects in High Performance P-Channel CCDs", IEEE Trans. Nucl. Sci., vol. 52, no. 6, pp. 2695-2702, 2005.

[13] Dawson, K., C. Bebek, J. Emes, et. al., "Radiation Tolerance of Fully-Depleted P-Channel CCDs Designed for the SNAP Satellite", IEEE Trans. Nucl. Sci., vol. 55, no. 3, pp. 1725-1735, 2008.

[14] J. P. D. Gow, N. J. Murray, A. D. Holland, et al., "Comparison of proton irradiated P-channel and N-channel CCDs", NIM A, vol. 686, pp. 15-19, 2012.

[15] D. H. Lumb, "CCD radiation damage in ESA Cosmic Vision missions: assessment and mitigation", *Proc. SPIE*, 2009, vol. 7439.

[16] J. Janesick, "Charge Transfer" in *Scientific Charge-coupled Devices*, SPIE Press, 2001, pp. 418 and 430.

[17] N. J. Mostek, C. Bebek, Karcher A., et al., "Charge trap identification for proton-irradiated p+ channel CCDs", *Proc. SPIE*, 2010, vol. 7742.

[18] W. Shockley and W. T. Jr. Read, "Statistics of the Recombination's of Holes and Electrons", Physical Review 87(5), pp. 835-842, 1952.

[19] R. N. Hall, "Electron-Hole Recombination in Germanium", Physical Review 87(5), pp. 387-387, 1952.

[20] G. R. Hopkinson, C. J. Dale, and P. W. Marshall, "Proton Effects in Charge-Coupled Devices", IEEE Trans. Nucl. Sci., vol. 43, pp. 614-627, 1996.